arXiv:cond-mat/9704044v1 [cond-mat.mes-hall] 4 Apr 1997

NMR lineshape in Metallic Nanoparticles: a Matrix Continued Fractions evaluation

Horacio M. Pastawski and José A. Gascón
Faculdad de Matemática, Astronomía y Física, Universidad Nacional de Córdoba, Ciudad Universitaria, 5000 Córdoba, Argentina

(2 december 1996)

In metallic nanoparticles, the different electronic environment seen by each magnetic nucleus produces a distribution of Knight shifts of the NMR frequencies which is observed as an inhomogeneously broadened lineshape. We study the fluctuations in the local density of states for s electrons at the Fermi energy in a simple LCAO model. We resort to a Matrix Continued Fractions calculation of the Green's functions. Results show that line broadens asymmetrically and its shift decreases as the particle size or the temperature diminish satisfying a universal scaling function. However, for very small particles, surface states become relevant to determine a lineshape that departs from the universal scaling behavior. These trends are consistent with the observed tendencies in Cu and Pt particles.

73.20.Dx, 76.60.Cq, 73.20.Fz

I. INTRODUCTION

Small clusters of atoms of metallic elements have interesting physical properties[1] which originate in the strong interference effects that appear when the coherence length L_ϕ of the electronic excitations is larger than the size L of the particle. As already noted by Kubo[2], this would allow the manifestation of the geometry dependent quantization of electron energies. This condition leads to the very active field of mesoscopic physics[3] which involves a deep revision of traditional ways of calculation and interpretation of transport and spectroscopic[4] properties. On the other hand the diverse technical applications of metal particles as well as composites of metal particles has pushed the development of a wealth of sample preparation techniques[17] which allow varied system characteristic. It has been recognized[5,6,7] that NMR can be a useful tool to characterize metallic nanoparticles and that further insight in the comprehension of their properties requires the development of models which allow a quantification of spectra. Such a model should contain the basic physics involved: Each magnetic nucleus is sensitive to *local* magnetic polarization of electrons which changes the effective field. This manifests[8] as different (Knight) shifts in the NMR absorption frequencies leading to inhomogeneous line broadening and different relaxation times. While it is obvious that a close connection exists between the output of an NMR experiment and the geometry and disorder of the particle on which the electronic properties depend, we are still far from a universal quantitative description of the effect.

In this paper we address the problem of how the size of a particle contributes to the NMR lineshape. Because of quantum interferences, the details of shape and disorder of the nanoparticles manifest[9,10] as a Wigner-Dyson or Poisson distribution of electronic energy levels depending on whether the states are extended (metallic phase) or localized (dielectric phase). In both cases, there are strong fluctuations in the local density of states (LDOS) and hence in the local Pauli susceptibility. Since samples used in earlier experiments had a distribution of particle sizes, the inhomogeneous line shapes were assigned to this distribution. Different sizes would not only give a different number of electrons at the Fermi energy (average density of states) but also involve a fluctuation in the parity of total electron number giving a further contribution to the inhomogeneity. However, these efforts, based in a canonical ensemble, do not give a consistent explanation for the observed lineshape valid for all the systems studied. A recent *break-through* was proposed[11] with the use of grand canonical ensemble which allows for fluctuations in the particle charge. This picture, which is valid in many experimental situations, emphasizes the fact that inhomogeneities manifest already in a single particle. Therefore inhomogeneous broadening occurs even when particles are exactly equal. This is observed[7] for the ligand-stabilized metal-cluster compounds $Pt_{309}Phen^*_{36}O_{30}$. Estimations of this shape were performed using an electronic structure represented by a non-linear sigma model[11] and by a Random Matrix Theory (RMT)[12]. Both models produce the same results for the LDOS fluctuations. One could visualize the model Hamiltonian implicit in the RMT theory, considering a set on M "atomic orbitals" whose interactions, not constrained to a given lattice, are described by the Hamiltonian matrix elements $\mathcal{H}_{i,j}$, which are random and satisfy a gaussian distribution $P(\mathcal{H}) = C\exp[-\mathrm{Tr}\mathcal{H}^2/(2\sigma^2)]$, with C a normalization constant and $\sigma^2 \sim M$ to keep a finite band width B. Since the analytical solutions are obtained in the limit $M \to \infty$, each "orbital" sees an equivalent "mean field" environment. While solutions describe fluctuations in the LDOS, they can not distinguish surface from bulk "orbitals" or the explicit geometry of the particles neither describe the transition to the localized regime. Hence, while these analytical models contain the essential physics of level statistics, they are not expected to provide a detailed characterization of different materials and particle geometries. In order to overcome

this limitation, in this work we use a very simple tight binding model for the electronic structure that is a first step toward a more precise description of the nanoparticles in terms of Linear Combination of Atomic Orbitals (LCAO). A similar model was used recently[9,10] to describe the cross over between Wigner-Dyson and Poisson statistics. We will also show that resorting to appropriate calculation tools (e.g. Matrix Continued Fractions) such models can be used in practical calculations.

II. THE MODEL

The electronic system is described by the Hamiltonian

$$\mathcal{H} = \sum_{i=1}^{M} E_i c_i^+ c_i + \sum_{j>i}^{M} \sum_{i=1}^{M} (V_{j,i} c_j^+ c_i + V_{i,j} c_i^+ c_j) \qquad (1)$$

where E_i is the energy of the s-like atomic state centered at nuclei position $\mathbf{r}_i$ orthogonalized atomic orbital $\varphi_i(\mathbf{r}) \equiv \varphi(\mathbf{r} - \mathbf{r}_i)$, and $V_{j,i}$ are real numbers accounting for the kinetic energy of the electrons. There are $M = \Omega/a^3$ orbitals in the volume $\Omega = L_1 L_2 L_3$. To model the disorder we assume that E_i's are uniformly distributed around the mean value E_S in the range $[-W/2, W/2]$ (Anderson model). In a Hartree mean field description, charge transfer energies are accounted for conserving the structure of (1). The presence of the magnetic field H leads to the unitary symmetry and can be included in the Hamiltonian through the Peierls substitution. However, for experimentally accessible fields ($H \leq 10^5$G) and typical particle sizes ($L \geq 10^{-7}$cm) its effect is negligible ($HL^2 e/(ch) \ll 1$ with $e/(ch) = 2.4 \times 10^6 \mathrm{G}^{-1}\mathrm{cm}^{-2}$) because degeneracies are already broken by the disorder and we restrict our calculation to orthogonal symmetry. In principle, interactions with other particles produce a decay of the eigenstates and enter through an inhomogeneous broadening of the ionization energy of orbitals at surfaces[13] ($E_i \to E_i - \mathrm{i}\Gamma_i$), accounting for electron tunneling toward neighbor particles. While this is not much complication in a numerical treatment of the problem, to allow for comparison with previous works, we adopt here a simpler description in which $\Gamma_i \equiv \eta_o$ at every site. Properties of the single particle excitation spectrum are contained in the retarded (advanced) Green's function

$$G_{i,j}^{R(A)}(\varepsilon) = \sum_k \frac{a_k(i) a_k^*(j)}{\varepsilon + [(-)\mathrm{i}\eta - E_k]}, \qquad (2)$$

where $\psi_k(\mathbf{r}) = \sum_i a_k(i)\varphi_i(\mathbf{r})$ and E_k are the exact eigenfunctions (molecular orbitals) and eigenenergies for the isolated particle. η is a natural broadening of the electronic states and the $(-)$ sign corresponds to the retarded Green's function. The local densities of states per atom (LDOS) at i-th site is evaluated as:

$$N_i(\varepsilon) = -(2\pi\mathrm{i})^{-1}[G_{i,i}^R(\varepsilon) - G_{i,i}^A(\varepsilon)], \qquad (3)$$

from which the relevant contribution to the density of states per unit volume at the i-th nucleus, $N(\varepsilon, \mathbf{r}_i)$, is obtained. In presence of an external magnetic field, electrons polarize proportionally to a *local* Pauli susceptibility

$$\chi_P(\mathbf{r}_i) = 2(g\mu)^2 \int N(\varepsilon, \mathbf{r}_i)[-\frac{\partial \mathrm{f}}{\partial \varepsilon}]\mathrm{d}\varepsilon, \qquad (4)$$

with $\mathrm{f}(\varepsilon)$ is the Fermi function. Numerical integration of (4) for finite temperatures can be very time consuming due to the singular nature of the spectrum which would require a LDOS calculation for each energy. In order to avoid integration, the finite temperature effects can be taken into account by taking

$$-[\frac{\partial \mathrm{f}}{\partial \varepsilon}] \approx \frac{1}{\pi} \frac{a_T k_B T}{(\varepsilon - \varepsilon_F)^2 + (a_T k_B T)^2}. \qquad (5)$$

which in practice becomes equivalent to put $k_B T = 0$ in Eq.4 and use an energy uncertainty for the electronic levels

$$\eta = \eta_o + k_B T, \qquad (6)$$

where the coefficient $a_T \equiv 1$ gives a good approximation approximation for Eq. (5). The Knight shift at a given nucleus is

$$\Delta\omega(\mathbf{r}_i) = J \frac{1}{g\mu} \chi_P(\mathbf{r}_i) H, \qquad (7)$$

where J is the hyperfine constant and $g\mu$ the electron magnetic moment. Then, $\Delta\omega(\mathbf{r}_i)$ will follow a probability distribution proportional to that of the electron LDOS. The NMR absorption line is inhomogeneously broadened by this distribution and is obtained by summing up all magnetic nuclei. The resonance line finally becomes

$$I(\omega) = A \sum_i \delta[\omega - \omega_0 - \Delta\omega(\mathbf{r}_i)], \qquad (8)$$

where ω_0 is the non-shifted position of the resonance in a dielectric material (as in a salt). That is, the observed NMR line shape is the sum of narrow lines with and inhomogeneously distribution in frequencies that follows that of the LDOS. In order to allow comparisons between systems, it is convenient to define the adimensional frequency variable $x = (\omega - \omega_o)/(\omega_K - \omega_o)$, where ω_K is the peak resonance in the bulk metal. This gives $x = 1$ for a metal and $x = 0$ for the dielectric phase.

The intensity can be normalized: $\int I(x)\mathrm{d}x = 1$. A quantity of interest to characterize the line is the Knight shift x_m defined as $I(x_m) = \max[I(x)]$; another is the first moment $x_1 = \int x I(x)\,\mathrm{d}x$, whose difference from x_m is a measure of the asymmetry of the line. Notice that if we are working within a grand canonical ensemble in an infinite system, we expect that even when an electronic density at some nuclei is diminished by interferences this is compensated by an increase in others. In the analytic

models[11] this property results in $x_1 = 1$. However in a MO model of the cluster this is not necessarily true. In a cluster, the ensemble average DOS is not a monotonic function of energy but an oscillating function with local maxima at the eigenenergies of the ordered cluster. This dependence on on the cluster size is an easy analytical result[14] for a Lorentzian distribution of site energies.

III. MATRIX CONTINUED FRACTION

The exact solution of Hamiltonian (1) is a formidable task. Rough features of the LDOS can be obtained by the Recursion Method[15]. This involves the obtention of a tridiagonal basis for (1) and the evaluation of the local Green's function (2) as a continued fraction. When used within the RMT this method allows analytical solutions[16]. We resort to it for the evaluation of the density of states per orbital in an infinite ordered system, $N_0(\varepsilon_F, \eta)$. From this quantity the typical level separation for a cluster with M orbitals is calculated:

$$\Delta = 1/[M \cdot N_0(\varepsilon_F, \eta)]. \tag{9}$$

However, for small η (low temperature), it is difficult to obtain the precise fluctuations in the LDOS for finite clusters, because the intrinsic numerical instabilities[17,18] of the tridiagonalization procedure distort the fine details of the LDOS[19]. It is therefore compelling to resort to a more robust method to describe the infinitesimal details of the density of states. This is the Matrix Continued Fractions (MCF) method[20] for the calculation of the local Green's function. Its basic idea is to exploit the short range interactions in Hamiltonian (1) by indexing states in a way that subspaces representing layers interact through nearest neighbor subspaces. In matrix form:

$$\mathcal{H} = \begin{bmatrix} \ddots & \ddots & \mathbf{0} & \mathbf{0} & \mathbf{0} \\ \ddots & \mathbf{E}_{n-1,n-1} & \mathbf{V}_{n-1,n} & \mathbf{0} & \mathbf{0} \\ \mathbf{0} & \mathbf{V}_{n,n-1} & \mathbf{E}_{n,n} & \mathbf{V}_{n,n+1} & \mathbf{0} \\ \mathbf{0} & \mathbf{0} & \mathbf{V}_{n+1,n} & \mathbf{E}_{n+1,n+1} & \ddots \\ \mathbf{0} & \mathbf{0} & \mathbf{0} & \ddots & \ddots \end{bmatrix}, \tag{10}$$

where $\mathbf{0}$'s are null matrices, $\mathbf{E}$'s in the diagonal represents intra-layer interactions while the only non-zero off-diagonal matrices and $\mathbf{V}_{n,n\pm1}$ connect nearest neighbor layers. Detailed structure of the submatrices depends on the lattice, for the cubic structure $\mathbf{V}_{n,n\pm1} = V\mathbf{1}$, with $\mathbf{1}$ the identity matrix. The local retarded Green's functions connecting sites i and j within the n-th layers are arranged in a matrix

$$\mathbf{G}^R_{n,n}(\varepsilon) = \left[(\varepsilon + \mathrm{i}\eta)\,\mathbf{1} - \mathbf{E}_{n,n} - \mathbf{\Sigma}^{R+}_n(\varepsilon) - \mathbf{\Sigma}^{R-}_n(\varepsilon)\right]^{-1} \tag{11}$$

where the matrix self energies $\mathbf{\Sigma}^{R+}_n$ and $\mathbf{\Sigma}^{R-}_n$ are calculated in terms of Matrix Continued Fractions (MCF) defined through the recurrence relations:

$$\mathbf{\Sigma}^{R\,\pm}_n = \mathbf{V}_{n,n\pm1} \frac{\mathbf{1}}{(\varepsilon + \mathrm{i}\eta)\,\mathbf{1} - \mathbf{E}_{n\pm1,n\pm1} - \mathbf{\Sigma}^{R\,\pm}_{n\pm1}} \mathbf{V}_{n\pm1,n}, \tag{12}$$

which are calculated with the boundary conditions: $\mathbf{\Sigma}^{+}_{L_3} \equiv \mathbf{\Sigma}^{-}_1 \equiv \mathbf{0}$. The intrinsic stability of the method manifests[21] in the fact that a modification of a layer at distance L away from a given one will produce an exponentially small variation of the local density of states, $\delta N \sim \exp[-\gamma_1 L]$. Here γ_1 is the minimum Lyapunov Characteristic Exponent. In the localized regime ($W > W_C$, $\eta = 0$) $1/\gamma_1$ coincides with the localization length while in the ordered case ($W \ll W_C$, $\eta > 0$) it gives a phase breaking length[14] $L_\phi(\eta)$ which washes out the finite size effects when $L > L_\phi$.

IV. RESULTS

In this work we consider a simple cubic structure forming clusters of cubic shape with sizes L ranging from 5 to 15 layers. That makes clusters of up to 3375 orbitals. We chose an arbitrary Fermi energy $\varepsilon_F = E_S + 4\,|V|$ which is far enough from the van Hove singularities for that lattice and hence allows a comparison with results from the non-linear sigma model which implies nearly free electrons. However, with $-V \approx 1e\mathrm{V} = 1.16 \times 10^4\mathrm{K}$, it gives a reasonable scale to describe an s metal such as Cu. Disorder is small enough ($W = 0.5\,|V|$) to be on the metallic side of the metal insulator transition but strong enough to provide randomness of the energy levels. Further sampling is achieved by considering an ensemble of 10 Fermi energies in a range $\delta\varepsilon_F = 0.5\,|V|$. This minimizes the effect of finite size correlations in the electron energy spectrum.

Figure 1 shows the normalized distribution of LDOS for a cluster of size L=15 with three temperatures producing effective broadenings $\eta/V = 0.05$, 0.0067 and 0.001; which according to Eq. (6) can be interpreted as a sequence of decreasing temperatures. The number of occurrences $I(x)$ of each normalized density of states

$$x = \frac{N_i(\varepsilon_F, \eta)}{N_0(\varepsilon_F, \eta)} \tag{13}$$

is proportional to the NMR absorption. Each member of the ensemble, containing four disorder configurations, is normalized according to the corresponding Fermi energy and line broadening, a dependence writen explicitly in Eq.(13). The same results were obtained with a single cluster, since the system is big enough to provide a configurational average. It is clear that by lowering the temperature the Knight shift decreases from its metallic limit $x_m = 1$ toward $x_m = 0$ corresponding to a salt.

Simultaneously the line becomes increasingly asymmetric. These results are consistent with the experiments in Cu[5][22] and Pt[6].

In Fig. 2 we show the variation of the lineshape with cluster sizes (L=10, 8 and 6) for a fixed natural broadening of $\eta/V = 0.018$. Again it confirms the general trend experimentally observed in Cu and the predictions of the analytical models, i.e. the band tends to broadens and maxima shift to lower frequencies as particle size or temperature is decreased.

In order to capture the universal nature of the competition between cluster size and temperature suggested by Figs. (1) and (2), we plot in Fig. (3) the value of the adimensional Knight Shift as a function of the scaling parameter $\eta/\Delta \equiv \alpha/(2\pi)$ which measures the ratio between the level broadening and the typical level separation. α is the scaling parameter defined in ref. [11]. For completeness we also include in the plot a continuous curve obtained from the analytical lineshape obtained in that work for the unitary ensemble. As expected for a given η/Δ their results tend to give a higher x_m than our numerical values. This is consistent with the fact that the breaking of time reversal symmetry produces a stronger level repulsion diminishing the fluctuations.

However, there is no universal scaling function that fits the complete lineshape for all systems. This is because in our model there are surfaces. Although we did not assign different ionization energies to surface orbitals (which can produce Tamm states), local densities of states at surface region (about $6/L$ of the total) can differ substantially from that at inner atoms[23]. Sites at the surfaces are connected to fewer neighbors and this manifest on a decrease in the wings of the LDOS as a consequence of lower gain in kinetic energy[24], which is compensated with an increase of the LDOS at energies around E_S. It should be emphasized, however, that the sign of the change in the LDOS at surfaces depends both, on the lattice structure and on the value of ε_F; e.g. if $\varepsilon_F = E_S$ the surface LDOS would be higher than its value in the bulk. In any case, this produces an additional fluctuation in the LDOS which is more important for smaller systems. These effects attenuate within a few lattice constants and are consistent with the exponential healing length model[25]. In Fig. (4) we separate the contributions to the distribution of LDOS (linewidth) from surface and inner sites in a small cluster. Similar separations of maxima are obtained at higher η/Δ. To emphasize the importance of this effect on the line broadening in small particles, we show in Fig.(5) the scaling function satisfied by x_m as function of the adimensional parameter η/Δ for a $5 \times 5 \times 5$ cluster in which we also discriminate the contributions of surface and inner sites. It is clear a general tendency toward lower values of the Knight shift for nuclei at the surfaces. Maxima do not coincide even when η/Δ is increased. In small clusters this effect manifests as an intrinsic linewidth persisting at high temperatures, a tendency that departs from the scaling law. This is the situation observed in recent experiments[26][27] on Pt_{309} and $Ni_{38}Pt_6$ particles, where linewidths do not shrink with increasing temperature. Our results suggest that size and temperature dependence of line shapes can be used in conjunction with other NMR techniques such as SEDOR[6] to allow the experimental identification of electronic densities at surface regions.

V. FINAL REMARKS

, In agreement with analytical theories[11][12] for mesoscopic fluctuation, our results show that distribution of LDOS (and hence NMR line) shifts and asymmetrically broadens as temperature decreases and particle size diminishes and can be described by a universal scaling law which is consistent general trends observed in Cu particles and the size dependence[26][27] of Pt_{309} and $Ni_{38}Pt_6$ particles, although the origin of the disorder in the last cases is not quite clear. In this case a finite broadening is obtained even for high temperatures. These departures from scaling theory in very small particles, is understood in our model as due to the presence of surfaces, a feature that the analytical theories do not contain. Therefore, our LCAO model contains the main features of mesoscopic fluctuations and models the exponential healing of surface effects. Due to the simplicity and speed of the MCF calculation, it allows for further improvements of the model Hamiltonian which should lead to a more detailed evaluation of the electronic structure. Also orbital susceptibility could be quantified within these models. Since Cu has also a contribution to the linewidth due to quadrupolar interactions, and Pt, having a d-band contribution to the Fermi surface, has an important core polarization susceptibility, they are far from ideal systems. A good candidate for a full quantification the described behavior is Ag, with spin 1/2 nucleus and s electrons. Therefore, further development along these lines would allow for: 1) a better quantification of NMR experiments; 2) the investigation of the electron states determining the chemical kinetics at surfaces and 3) the progress in the understanding of basic phenomena at a mesoscopic scale. While the first issue was the main one addressed in this article we would like to add a few comments on the other two. Since in a frontier-orbital picture of bonding to metal surfaces, the states around the Fermi energy are those that determine the chemical reactions, it is of great interest to determine how these are modified by changing the size and disorder of the catalyst particle[28]. In particular a metal-insulator transition in the low dimensional (Tamm) surface band could play a very relevant role in chemical kinetics. Therefore, the theoretical and experimental methods described in this paper can be conveniently adapted to suit this investigation. Finally, the interference phenomena lying in the core of mesoscopic physics could be controlled to obtain a fine tuning of many static and dynamical properties of materials. In particular, the present technique could be used to com-

plement current studies[10] that attempt to quantify the interplay of disorder, magnetic field and temperature in the metal-insulator transition.

VI. ACKNOWLEDGMENTS

This work was performed at LANAIS de RMN (UNC-CONICET) with financial support from Fundación Antorchas, CONICOR and SeCyT-UNC. HMP is a member of CONICET and appreciates discussions with H. Brom, C. Beenakker, V. Prigodin and K. Efetov.

[1] W. P. Halperin, Rev. Mod. Phys. **58**, 533 (1986)
[2] R. Kubo, J. Phys. Soc. Japan **17**, 976 (1962)
[3] B. L. Altshuler, P. A. Lee and R. A. Webb (eds.), *Mesoscopic Phenomena in Solids*, (North-Holland Amsterdam, 1991)
[4] H. M. Pastawski, P. R. Levstein and G. Usaj, Phys. Rev. Lett.**75**, 4310 (1995); H. M. Pastawski, G. Usaj and P. R. Levstein, Chem. Phys. Lett. **261**, 329 (1996)
[5] P. Yee and W. D. Knight, Phys. Rev. B, **11** 3261 (1975)
[6] C. D. Makowka and C. P. Slichter, Phys. Rev. B **31**, 5663 (1985)
[7] H. B. Brom, D. van der Putten and J. L. de Jongh, in *Physics and Chemistry of Metal Clusters* L. J. de Jongh ed., Kluwer Academic Publishers (Netherlands, 1994)
[8] C. P. Slichter, *Principles of Magnetic Resonance* (Springer, New York 1990)
[9] I. Kh. Zharekeshev and B. Kramer, Phys. Rev B **51**, 17 239 (1995)
[10] M. Batsch, L. Schweitzer, I. Kh. Zharekeshev and B. Kramer, Phys. Rev. Lett. **77**, 1552 (1996)
[11] K. B. Efetov and V. N. Prigodin, Phys. Rev. Lett. **70**, 1315 (1993)
[12] C. W. Beenakker, Phys. Rev. B, **50**, 15170 (1994)
[13] H. M. Pastawski, Phys. Rev. B **44**, 6329 (1991); **46**, 4053 (1992);J. L. D'Amato and H. M. Pastawski, Phys. Rev. B **41**, 7411 (1990)
[14] D. Rodrigues, H. M. Pastawski and J. F. Weisz, Phys. Rev. B **34**, 5459 (1986)
[15] R. Haydock, V. Heine and M. J. Kelly, J. Phys. C **5** 2845 (1972); **8**, 2591 (1975); see also Solid. St. Phys. **35** (1980)
[16] D. C. Mattis and R. Raghavan, Phys Lett. A **75**, 3313 (1980)
[17] R. Haydock, Computers Physics Communication, **30**, 221 (1983)
[18] J. K. Cullum and R. A. Willoughby,*Lanczos Algorithms for Large Symmetric Computations*, Vol I, (Birkhäuser)
[19] H. M. Pastawski, J. A. Gascón and E. Medina, Anales Asoc. Quím. Arg. (in press) (1996)
[20] H. M. Pastawski, J. F. Weisz and S. Albornoz, Phys. Rev. B **28**, 6896 (1983)
[21] H. M. Pastawski, C. Slutzky and J. F. Weisz, Phys. Rev. B Phys. Rev. B **32**, 3642 (1985)
[22] S. Kobayashi, T. Takahashi and W. Sasaki, J. Phys. Soc. Jpn **31**, 1442 (1971); **32**, 1234 (1972)
[23] J. R. Schrieffer and P. Soven, Physics Today, **29**(4) 26 (1975); D. Kalkstein and P. Soven, Suf. Science **26**, 85 (1971)
[24] H. M. Pastawski and C. Wiecko, Phys. Rev. A **36**, 5854-8 (1987)
[25] Y. Y. Tong and J. J. van der Klink, J. Phys.: Condens. Matter **7**, 2447 (1995)
[26] D. van der Putten, H. B. Brom, J. Witteveen, L. J. de Jongh and G. Schmid, Z. Phys. D **26**, S21 (1993)
[27] H. B. Brom, J. J. van der Klink, F. C. Fritschij, L. J. de Jongh, R. Della Pergola and A. Ceriotti, Z. Phys. D **in press** (1996)
[28] R. Hoffmann, J. Phys. Condens. Matter, **5** A1 (1993).

VII. FIGURE CAPTIONS

Figure 1. Typical distribution of occurrences I of LDOS (or NMR lineshape) as function of the adimensional frequency $x = (\omega - \omega_0)/(\omega_K - \omega_0) = N(\varepsilon_F, \eta)/N_0(\varepsilon_F, \eta)$ evaluated for an ensemble of 4 clusters of $15 \times 15 \times 15$ orbitals sampling 10 energies around $\varepsilon_F = E_s + 4\,|V|$ at different temperatures: $\eta/V = \eta_o + k_B T = 0.05$, 0.0067 and 0.001 The disorder is $W = 0.5\,|V|$.

Figure 2. Variation of NMR lineshape I for an ensemble of 10 particles of sizes $L = 6$, 8 and 10 lattice units, with 10 energies each. Temperature is such that $\eta = 0.018\,|V|$, and other parameters are as in Fig. (1).

Figure 3. Scaling curve for the Knight shift x_m for particles of different sizes as function of the adimensional parameter η/Δ. The continuous curve is obtained from the analytical solution for a unitary ensemble of ref.[11].

Figure 4. Surface and bulk contribution to the line shape in a small cluster ($M = 5 \times 5 \times 5$), calculated with an ensemble of 20 different disorder configuration and 10 energies each. Temperature is such that $\eta/V = 0.031$. The dotted plot corresponds to normalized contributions of orbitals in the surface of the cluster. Full line plot is from inner sites.

Figure 5. Surface and Bulk contribution to the Knight shift (or maximum in the line) is shown here for a small cluster with varying $\eta/V = \eta_o + k_B T$ evaluated from curves as those in Fig. (4). Open triangles represent inner nuclei while open circles are those on the surface. Filled squares represent the Knight shift evaluated from all sites.

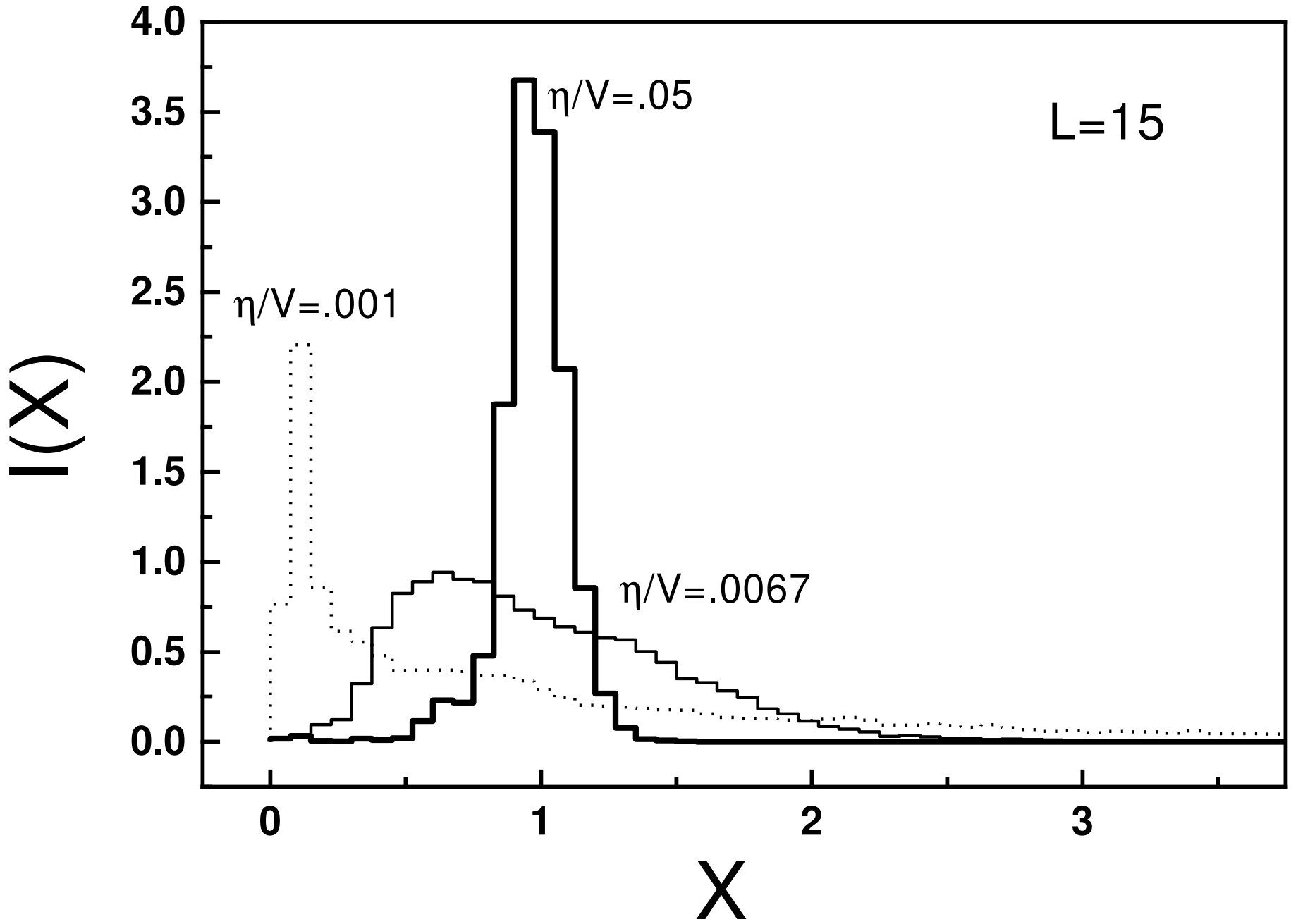
4.0
3.5
3.0
2.5
2.0
1.5
1.0
0.5
0.0
I(X)
η/V=.05
L=15
η/V=.001
η/V=.0067
0
1
2
3
X

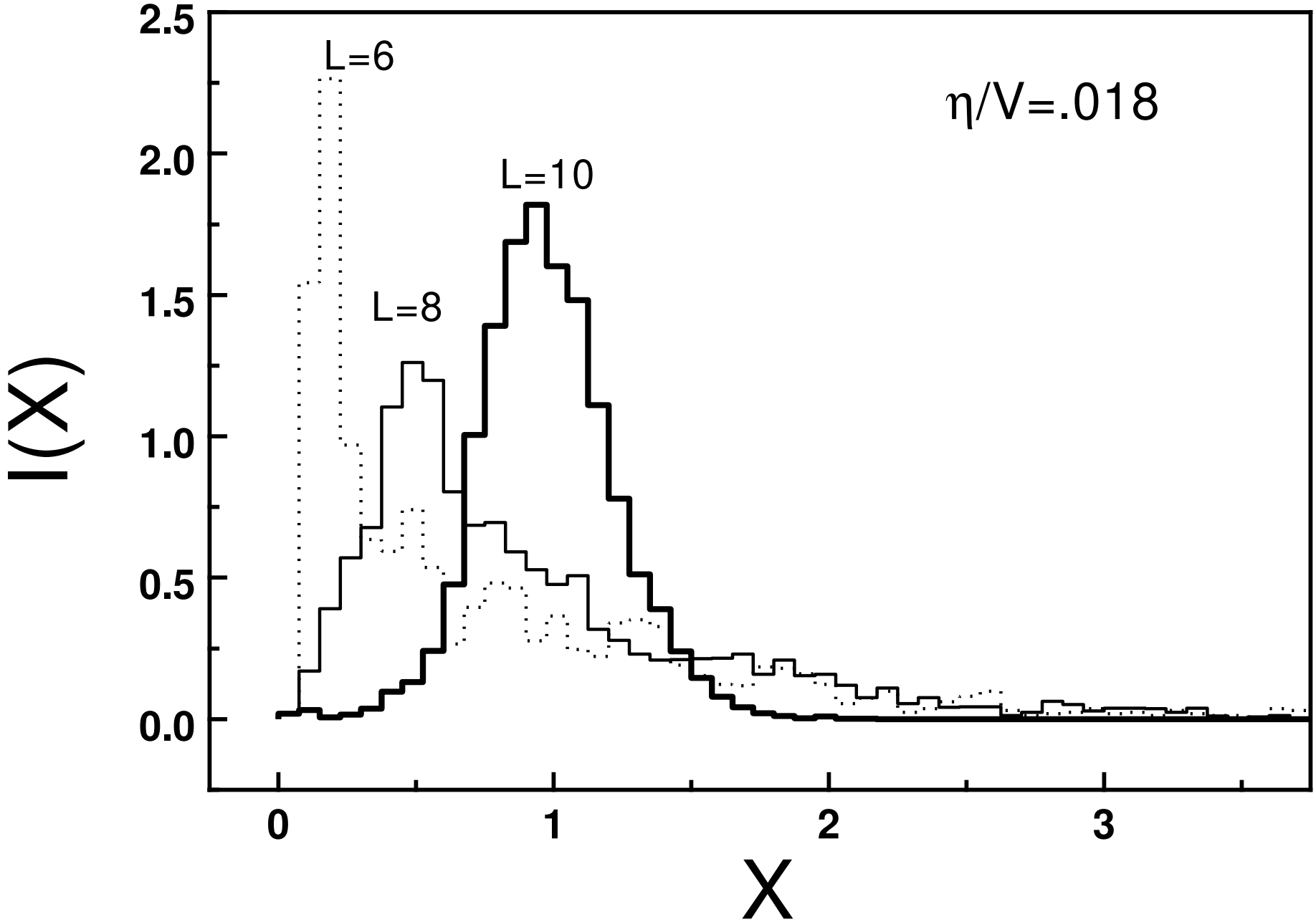
L=6
L=8
L=10
η/V=.018
I(X)
X
2.5
2.0
1.5
1.0
0.5
0.0
0
1
2
3

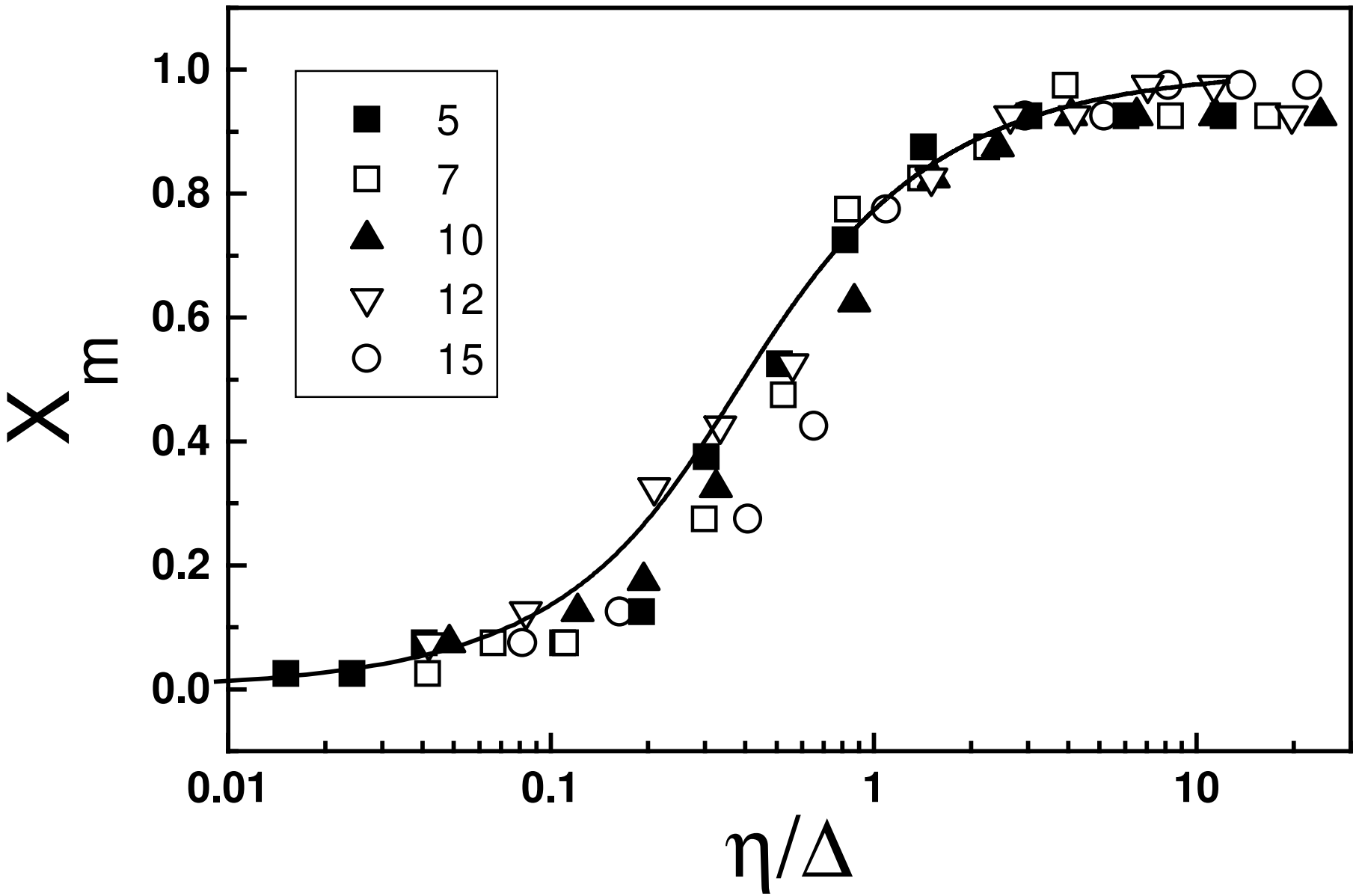
1.0
0.8
0.6
0.4
0.2
0.0
0.01
0.1
1
10
η/Δ
X m
5
7
10
12
15

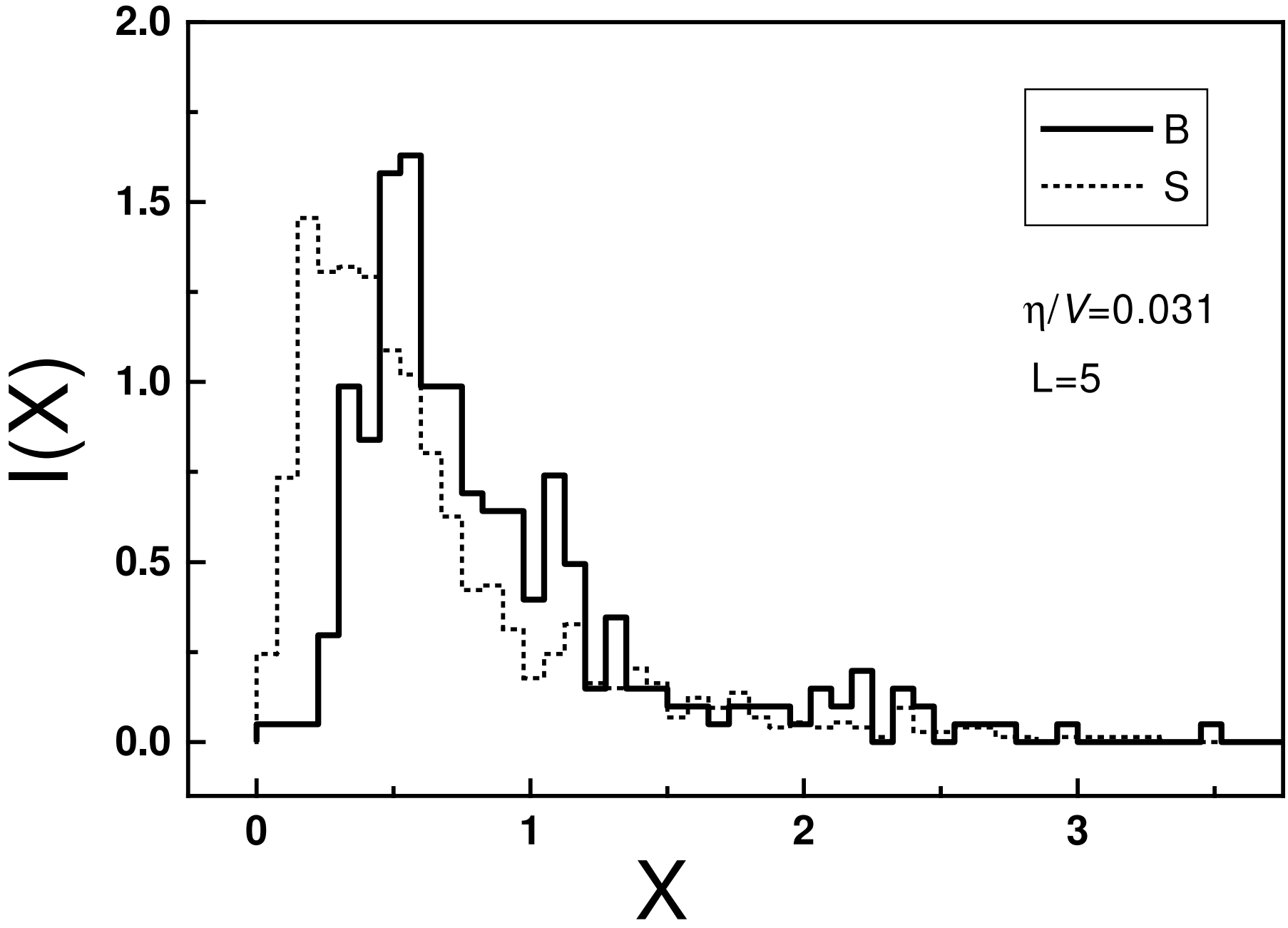
2.0
1.5
1.0
0.5
0.0
I(X)
0
1
2
3
X
B
S
η/V=0.031
L=5

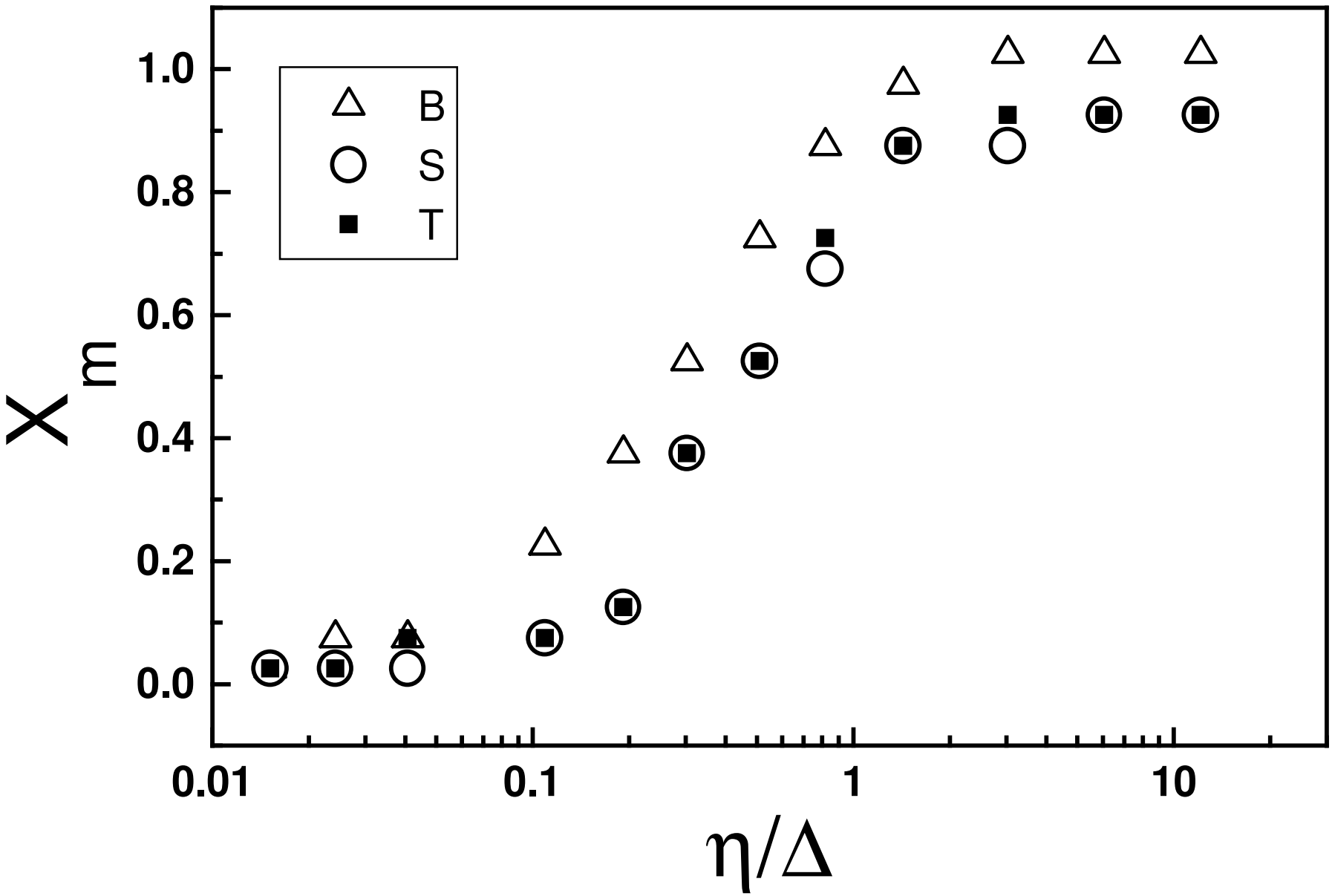
B
S
T
1.0
0.8
0.6
0.4
0.2
0.0
X_m
0.01
0.1
1
10
η/Δ